Topics in Catalysis Vol. 39, Nos. 3–4, October 2006 (© 2006)
DOI: 10.1007/s11244-006-0050-5

Reactivity of supported platinum nanoclusters studied by in situ GISAXS: clusters stability under hydrogen

Randall E. Winans[a,b,*], Stefan Vajda[a,c], Gregory E. Ballentine[a], Jeffrey W. Elam[d], Byeongdu Lee[b], Michael J. Pellin[e], Sönke Seifert[b], George Y. Tikhonov[a], and Nancy A. Tomczyk[a]

[a]*Chemistry Division, Argonne National Laboratory, 9700 South Cass Avenue, Argonne, IL 60439, USA*
[b]*X-ray Science Division, Argonne National Laboratory, 9700 South Cass Avenue, Argonne, IL 60439, USA*
[c]*Energy Systems Division, Center for Nanoscale Materials, Argonne National Laboratory, 9700 South Cass Avenue, Argonne, IL 60439, USA*
[d]*Energy Systems Division, Argonne National Laboratory, 9700 South Cass Avenue, Argonne, IL 60439, USA*
[e]*Materials Science Division, Argonne National Laboratory, 9700 South Cass Avenue, Argonne, IL 60439, USA*

This paper is an initial study of the reactivity and thermal stability of atomic platinum clusters supported on $Al_2O_3/SiO_2/Si(100)$ as a function of the thickness of the alumina film and presence of hydrogen. Extremely high thermal stability of Pt_{7-10} clusters *in vacuo* as well as in the presence of hydrogen is observed on $SiO_2/Si(100)$ coated with six cycles of Al_2O_3 film prepared by an atomic layer deposition technique.

KEY WORDS: platinum; supported clusters; size-selection; sintering; thermal stability; aggregation; support effect; atomic layer deposition; ALD film; GISAXS, hydrogen.

1. Introduction

Sintering of supported catalytically active nanoparticles during chemical reactions at elevated temperatures often leads to the loss of the catalytic activity and selectivity of these particles [1–3]. Previous studies of the thermal stability region on a sample of Pt nanoparticles formed upon deposition of non-size selected clusters at a surface coverage of $6.8\times10^{14}(\pm10\%)$ Pt atoms per cm^2 on $SiO_2/Si(111)$ (corresponds to 34% of one atomic monolayer) showed the onset of nanoparticle aggregation at around 320 °C [4]. Real-time studies of the Pt nanoparticle aggregation at 400 °C performed on a set of samples with varying initial nanoparticle sizes revealed a two-step agglomeration process with the first step completed within ~30 min [5]. This contribution is devoted to the study of the thermal stability of deposited size-selected platinum clusters by employing grazing incidence small angle X-ray scattering technique (GISAXS) exposed to hydrogen and in vacuum. Earlier studies on supported small metal clusters have demonstrated that under "soft-landing" conditions (kinetic energies of approximately 1 eV/atom or less), the clusters remain intact and do not undergo fragmentation upon impact on the surface [6–9]. In order to avoid cluster fragmentation during the deposition process, the upper kinetic energy limit was kept at 1 eV/atom. GISAXS can provide the same type of information as regular SAXS, but in addition, it can give depth profile information and particle–particle distances. Also, the aspect ratio (height/diameter) of a metal cluster can be calculated from the GISAXS data, and using the Wulff-Kaishew construction, the interfacial energy can be obtained [10]. It is ideal for *in situ* studies since it is very sensitive to surface species and there is less parasitic scattering resulting from the substrate compared to a direct transmission scattering experiment. The technique has become popular for studying quantum dots and clusters on, and imbedded into, surfaces. For instance, CdS quantum dots prepared from ion implantation of S and Cd in SiO_2 followed by annealing were characterized by GISAXS [11]. Variation of the size of the quantum dots (on the order of 4–5 nm) was determined as a function of depth. In a study of gold aggregates and carbon-platinum clusters, Naudon et al. [12] make an important point that this method samples a large area, yielding good statistics which is difficult to do with microscopy. They noted that clusters as small as 40 atoms were observed for the C–Pt clusters, and the anisotropy of the aggregates can be clearly resolved as well. Recent work of Renaud et al. [13] demonstrated the high sensitivity of the GISAXS technique to monitor in real time the growth of Pd clusters on MgO(100) and of Co on Au(111) during metal vapor deposition and this work has been extended to a quantitative study of the growth of Pd particles on MgO [10]. Also, GISAXS was used to characterize Au clusters deposited on a Si wafer which was covered by a C sub layer to make a comparison with TEM [14].

2. Experimental

2.1. Support material

As support material for size-selected clusters, thin alumina films (Al_2O_3 /SiO_2/Si(100)) prepared by atomic layer deposition (ALD) were used. ALD is a

* To whom correspondence should be addressed.
E-mail: rewinans@anl.gov

thin film growth method utilizing a pair of self limiting chemical reactions between gaseous precursor molecules and a solid surface to deposit films in a monolayer-by-monolayer fashion [15]. Exposing the surface to reactant A results in the self-terminating adsorption of a monolayer of A species. The resulting surface becomes the starting substrate for reaction B. Subsequent exposure to molecule B will cover the functionalized surface with a monolayer of B species. As a result, one AB cycle deposits less than one monolayer of the compound AB and regenerates the initial substrate. The SiO_2/Si(100) substrates were coated by Al_2O_3 ALD using alternating exposures to trimethyl aluminum (TMA, Aldrich) and deionized water in a viscous flow ALD reactor at a temperature of 200 °C [16, 17]. For these studies, alumina surfaces were produced with 2 and 6 ALD cycles

2.2. Cluster deposition

The continuous beam of platinum clusters was generated in a new high-flux laser vaporization cluster source which utilizes a Quantronix Nd YAG laser operating at 4.5 kHz (see figure 1). The beam of neutral and charged clusters passes through a biased skimmer into the ion guide of the second differentially pumped vacuum stage and then into the third stage. The positively charged clusters are guided and focused into the quadrupole mass spectrometer (Extrel) for mass analysis. Narrow cluster distributions in the size range Pt_n^+, $n = 1,...10$, with two to four dominant sizes can be produced by optimizing the temperature of the clusters source, pressure of the helium carrier gas and potential settings on the individual ion optics elements. After the desired cluster distribution is produced, by reversing the polarity settings on the quadrupole deflector, the cluster cations are deflected into an ion lens setup placed in front of the substrate mounted on a translation stage. The kinetic energy of clusters landing on the surface is controlled by biasing the substrate. Typical deposition energies are in the order of 1 eV/atom. The flux of clusters landing on the support is monitored in real-time using a picoammeter (Keithley). Typical deposition currents are in the order of tens to hundreds of picoamperes, depending on the size of clusters. Surface coverage of 2% of atomic monolayer equivalent (ML) was employed, with the goal of avoiding considerable aggregation of clusters into larger particles after they land on the surface. The size of the substrates was 18×15 mm^2. In order to improve the signal to background ratio in the GISAXS experiments, the covered surface area was increased by translation of the substrate during deposition. As a result, an approximately 3 mm $\times$ 10 mm surface area covered with clusters was obtained. All samples were prepared using the identical scheme, surface coverage and cluster size distributions consisting of Pt_{7-10}.

2.3. Grazing incidence small angle X-ray scattering (GISAXS)

The GISAXS experiments were performed in a vacuum chamber equipped with a heated sample holder mounted on a goniometer at the Advanced Photon Source (APS) BESSRC/XOR 12-ID-C beamline. During heat treatment, scattering data can be collected as a function of time and temperature. The beam was scattered off the surface of the sample at and near the critical angle ($\alpha_c = 0.15$) of the silicon substrate. The scattered X-rays were detected by a nine-element mosaic CCD detector [18]. The data was analyzed by taking cuts in the q_{xy} direction for horizontal information and in the q_z direction for vertical information (see figure 2). As a result, the anisotropy in particle shape can be determined [4, 5, 19–21].

3. Results and discussion

3.1. Pt_{7-10} clusters supported on Al_2O_3 (2 cycle)/SiO_2/Si(100)

Figure 3 shows 2-dimensional GISAXS images obtained on the two ALD cycle supported nanoparticles at room temperature, and after reaching 400 °C. Only

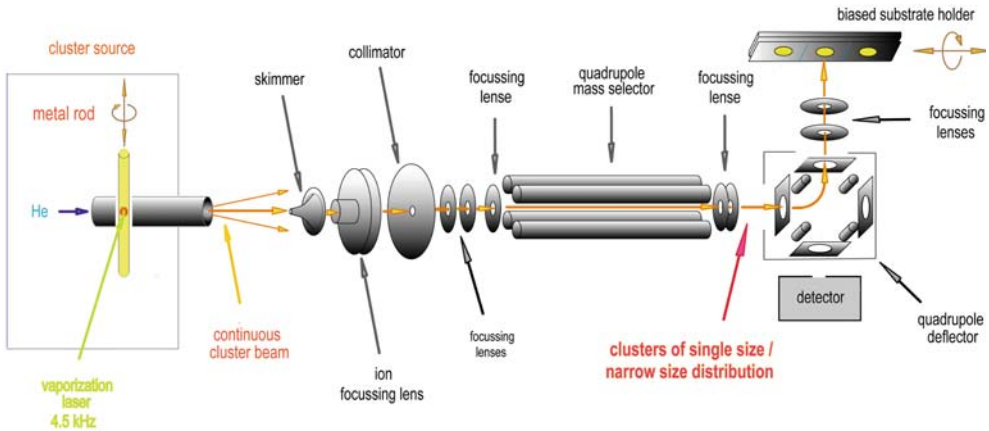

Figure 1. Schematic of the cluster deposition setup.

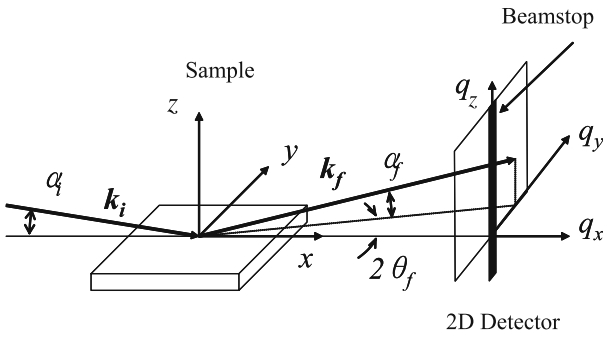

Figure 2. Schematic of GISAXS experiment: Incident X-ray beam (k_i) incident angle (α_i), and scattered beam and scattering (α_f). Scattering vectors q are calculated from $(4\pi/\lambda)\sin\theta f$ where θf is the scattering half angle and λ is the wavelength of the X-rays.

very weak scattering arising from small clusters is detectable at room temperature (figure 3a). The change in GISAXS pattern recorded at 400 °C clearly reflects the growth in particle size. The corresponding vertical

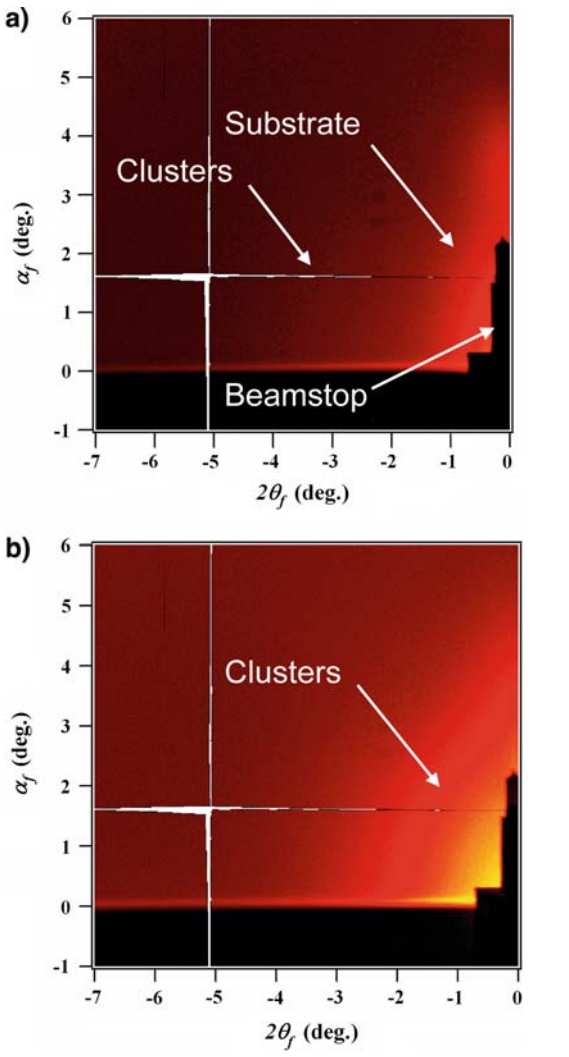

Figure 3. X-ray scattering data obtained on Pt_{7-10} clusters supported on 2 ALD cycles Al_2O_3 film on SiO_2/Si(100) in the absence of H_2 at room temperature (a) and at 400 °C (b).

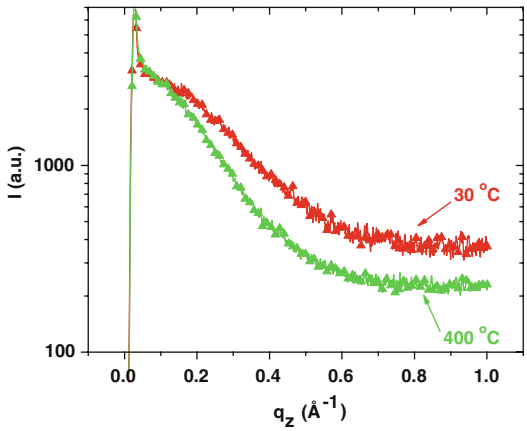

Figure 4. Background subtracted vertical cuts of AGISAXS data of Pt_{7-10} clustures on Al_2O_3 (2-cycle) /SiO_2/Si(100) in vaccum.

cuts of GISAXS data are shown in figure 4a and shows a change in particle height from R_g = 6–8 Å. (For a spherical particle, the relation between the radius of the particle R and the radius of gyration R_g resulting from Guinier analysis is defined as $R = 1.29 \times R_g$.). The evolution of platinum nanoparticle size and shape during the 4-h heat treatment is shown in figure 5a. The vertical (R_{gv}) and horizontal (R_{gh}) radii of gyration reflects the average height and width of the particles, respectively. Within the experimental error, R_{gv} and R_{gh} are identical at temperatures up to about 350 °C, thus indicating spherical particles. At 350 °C the onset of anisotropic 3-dimensional particle growth is observed, yielding oblate spheroids. When reaching 400 °C, R_{gv} and R_{gh} increases to 8 Å and 10.5 Å, respectively. Further heat treatment at a constant 400 °C for 25 min produces particles with R_{gv} = 9 Å and R_{gh} = 12.5 Å.

3.2. Pt_{7-10} clusters supported on Al_2O_3 (6 cycle)/SiO_2/Si(100)

In order to study the effect of surface composition and the effect of hydrogen, platinum clusters supported on 6 cycle Al_2O_3 film were heated in the absence and in the presence of hydrogen. The results are summarized in figure 6. Heat treatment with final the temperature reaching 400 °C does not lead to any noticeable change in particle size. The clusters preserved their small size (< 3 Å) both in the absence (figure 6a) and in the presence of hydrogen (figure 6b). However, the scattering from the 6-cycle Al_2O_3 substrate is much greater than seen in the case of the 2-cycle Al_2O_3 support film (figure 4.) The flat scattering patterns at $q_z > 5$ Å^{-1} reflects the small nature of the clusters. However, because of the substrate scattering, only an upper limit on the size can be determined. The value of 3 Å shown corresponds to 3 Å calculated for the largest cluster of Pt_{10} (see simulated data plotted in figure 6b) [22].

The extremely high stability of Pt clusters on the 6-cycle alumina film support compared to the 2-cycle

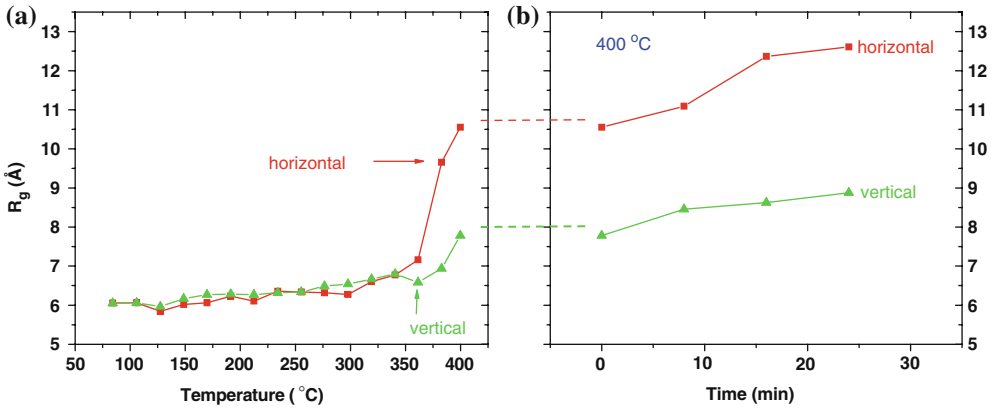

Figure 5. Changes of the average vertical and horizontal radii of gyration R_g of Pt_{7-10} clusters supported on 2 ALD cycles Al_2O_3 film on SiO_2/Si(100) in the absence of H_2. (a): temperature dependence and (b): kinetics monitored after reaching 400 °C.

film can be explained by the different structure of the ALD films. Our X-ray studies show that alumina films grow as islands and that a low number of cycles produces support with Al_2O_3 islands while leaving part of the underlying SiO_2/Si(100) surface naked [23]. With 2-cycle films, holes in the alumina film have been observed [23] which is in a good agreement with published results [24]. As shown in earlier studies on platinum and gold clusters, the particles are much more mobile on silica than on alumina (figure 7) [5]. The

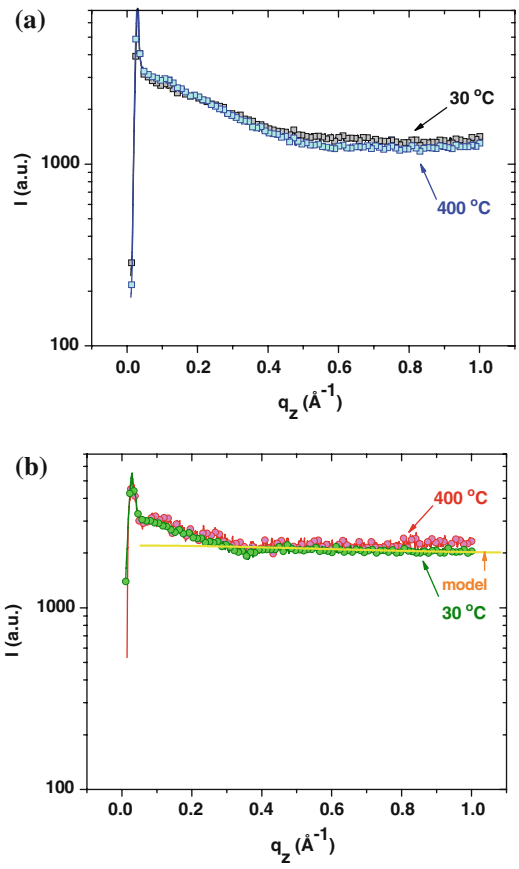

Figure 6. Background subtracted vertical cuts of AGISAXS data for Pt_{7-10} clusters on Al_2O_3(6-cycle) /SiO_2/Si(100) in the absence of H_2. (a) and in the presence of H_2 (b). The solid line in (b) shows the simulated GISAXS signal generated for monodispersed spherical Pt_{10} particles with 3 Å radius.

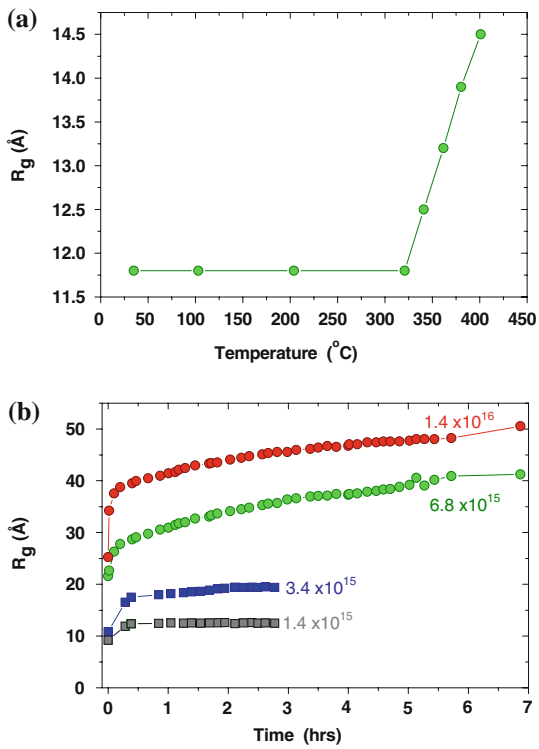

Figure 7. Pt nanoparticles formed from deposited non-size-selected clusters on SiO_2/Si(111). (a): Change in the average radius of gyration as a function of temperature for a sample with a level of surface coverage 6.8×10^{14} (±10%) Pt atoms/cm^2 (34% ML). Cluster aggregation has an onset around 350 °C. (b): Change in the radii of gyration of Pt nanoparticles at 400 °C as a function of time and surface coverage. The results indicates a two-step agglomeration process with the first step completed within ~30 min.

aggregation of platinum clusters on the 2-cycle alumina film is caused by migration, and subsequent coalescence, of Pt_n clusters initially more weakly bound to the silica surface. In contrast, the 6-cycle alumina film anchors the deposited particles and prevents their aggregation even when exposed to hydrogen. These results demonstrate new ways of synthesis of extremely stable supported nanocatalysts with atomic precision.

4. Summary

With the incomplete coverage of Al_2O_3 for two ALD cycles, the clusters appear to aggregate on the exposed Si/SiO_2 surface. Unprecedented thermal stability of $Pt_{7–10}$ clusters supported on six cycle Al_2O_3 film on SiO_2/Si(100) was observed. The clusters did not undergo aggregation during the lengthy heat treatment reaching 400 °C in vacuum and when exposed to hydrogen. This finding is in contradiction with the results obtained on gold clusters of same size, which undergo two- or three-dimensional growth under vacuum conditions and in the presence of hydrogen, respectively [21]. These experiments demonstrate the powerful combination of controlled size-selected cluster deposition, synchrotron and atomic layer deposition techniques, which can aid in design of new nanoparticle-support combinations with potential use in catalysis. Currently the approach is being used to study platinum and gold clusters as they are exposed to reactive gas mixtures at elevated temperatures and characterization of the support film structure. These studies will be extended to element specific studies on multi-component catalytic systems by using anomalous GISAXS.

Acknowledgments

The use of Advance Photon Source was supported by the US Department of Energy, Office of Basic Energy Sciences, and the study by OBES, Division of Chemical Sciences, Geosciences, and Biosciences under contract number W-31-109-ENG-38.

References

[1] B.K. Min, A.K Santra and D.W. Goodman, Catal. Today 85 (2003) 113.
[2] K. Hayashi, T. Horiuchi, K. Suzuki and T. Mori, Catal. Lett. 78 (2002) 43.
[3] Z.X. Chen, G.C. Smith, C.A.J. Putman and E.J.M. ter Voert, Catal. Lett. 50 (1998) 49.
[4] R.E. Winans, S. Vajda, B. Lee, S.J. Riley, S. Seifert, G.Y. Tikhonov and N Tomczyk, J. Phys. Chem. B 108 (2004) 18105.
[5] S. Vajda, R.E. Winans, J.W. Elam, B. Lee, M.J. Pellin, S.J. Riley, S. Seifert, G.Y. Tikhonov and N.A Tomczyk, Am. Chem. Soc., Div. Fuel Chem. 50 (2005) 190.
[6] U. Heiz, A. Sanchez and S Abbet, Eur. Phys. J. 9 (1999) 1.
[7] U Heiz, Appl. Phys. A 67 (1998) 621.
[8] S. Lee, C. Fan, T. Wu and S.L Anderson, J. Amer. Chem. Soc. 126 (2004) 5682.
[9] R. Schaub, H. Jödicke, F. Brunet, R. Monot, J Buttet and W Harbich, Phys. Rev. Lett. 86 (2001) 3590.
[10] C. Revenant, F. Leroy, R. Lazzari, G. Renaud and C.R Henry, Phys. Rev. B: Condens Matter Mater. Physics 69 (2004) 035411.
[11] P. Dubcek, S. Bernstorff, U.V. Desnica, I.D. Desnica -Frankovic and K Salamon, Surf. Rev. Lett. 9 (2002) 455.
[12] A. Naudon, D. Babonneau, D. Thiaudiere and S Lequien, Phys B: Condens Matter 283 (2000) 69.
[13] G. Renaud, R. Lazzari, C. Revenant, A. Barbier, M. Noblet, O. Ulrich, F. Leroy, J. Jupille, Y. Borensztein, C.R. Henry, J.-P. Deville, F. Scheurer, J. Mane-Mane and O Fruchart, Science 300 (2003) 1416.
[14] A. Naudon and D. Thiaudiere, J. Appl. Crystallogr 30 (1997) 822–827.
[15] S.M. George, A.W. Ott and J.W Klaus, J. Phys. Chem. 100 (1996) 13121.
[16] J.W. Elam, M.D. Groner and S.M. George, Rev. Sci. Instru. 73 (2002) 2981.
[17] J.W. Elam, Chem. Mater. 15 (2003) 1020.
[18] S. Seifert, R.E. Winans, D.M. Tiede and P. Thiyagarajan, J. Appl. Crystallogr. 33 (2000) 782.
[19] B. Lee, S. Seifert, S.J. Riley, G.Y. Tikhonov, N.A. Tomczyk, S. Vajda and R.E. Winans, Am. Chem. Soc., Div. Fuel Chem. 50 (2005) 188.
[20] B. S. Lee Seifert, S.J. Riley and G.Y. N. S. R.E. Tikhonov Tomczyk Vajda Winans, J. Chem. Phys. 123 (2005) 074701.
[21] S. Vajda, R.E. Winans, B.J.W. Elam, B. Lee, M.J. Pellin, S. Seifert, G.Y. Tikhonov and N.A. Tomczyk Topics in Catalysis (2006) in this volume.
[22] The estimated radius of the Pt_{10} cluster was obtained by assuming a spherical particle shape and Pt–Pt bond length of 2.775 Å.
[23] B. Lee, Vajda, Winans, to be published.
[24] R.L. Puurunen, J. Appl. Phys. 97 (2005) 121301.